Analysis of the net charge-compensation contribution in the fine structure of EPR defect centers: Cr^{3+}, Fe^{3+}, and Gd^{3+} in A_2MX_4-, AMX_3-, and MX_2-type crystals

Czesław Rudowicz
Research School of Chemistry, Australian National University, G.P.O. Box 4, Canberra A.C.T. 2601, Australia
(Received 21 April 1987)

The net charge-compensation (NCC) model recently proposed by us is applied to EPR defect centers: Cr^{3+}, Fe^{3+}, and Gd^{3+} in A_2MX_4-, AMX_3-, and MX_2-type crystals, where A is an alkali metal, M is an alkaline-earth metal, and X is a halide ion. The NCC model expresses the zero-field-splitting (ZFS) Hamiltonian for a charge-compensated center in terms of a ZFS Hamiltonian for a nonlocally compensated center and a ZFS Hamiltonian describing the net effect of charge compensation. This partition enables, using the transformation properties of the Stevens operators, extraction of the net contribution due to charge compensation. It is shown that the previous Takeuchi *et al.* model for charge-compensated Cr^{3+} ($S=\frac{3}{2}$) centers in A_2MF_4 is a particular case of a more general NCC model. Analysis of EPR data for the Cr^{3+} centers II (nearly trigonal) in A_2MF_4 and A_2MCl_4 crystals, in terms of our model, shows that the net charge-compensation contribution exhibits a significant monoclinic component neglected in the previous model. Numerical results for the ZFS parameters describing the net effect of charge compensation are given in the special axis system with $[b_2^1]=0$ and in the trigonal axis system. EPR data on trigonal and tetragonal Cr^{3+}, Fe^{3+}, and Gd^{3+} centers in AMF_3 crystals are also considered in terms of the NCC model. Discussion of the orthorhombic Gd^{3+} centers in MX_2 crystals indicates that the use of the "parameter shifts" by some authors, i.e., the differences between the rhombic and cubic parameters (referred to the same axis system), is equivalent to an implicit use of the NCC model. Expressions enabling application of the NCC model to EPR centers with higher spin, e.g., Fe^{3+} ($S=\frac{5}{2}$) and Gd^{3+} ($S=\frac{7}{2}$), in the crystals considered are provided.

I. INTRODUCTION

Recently the EPR data on charge-compensated Cr^{3+} ($S=\frac{3}{2}$) centers in several A_2MF_4- (A represents an alkali metal and M represents an alkaline-earth metal ion) type crystals of K_2NiF_4-like structure have been interpreted[1-3] in terms of a superposition of two uniaxial zero-field-splitting (ZFS) terms: $D_1S_z^2$ for a vacancy-free (i.e., nonlocally charge-compensated) Cr^{3+} center in A_2MF_4 and $D_2S_{z'}^2$ for the corresponding charge-compensated Cr^{3+} center in AMF_3. It seems worthwhile to apply and subsequently test the model[1] for the EPR centers with higher spin $S\geq 2$. To this end a derivation of the model formulas for the fourth- and sixth-order ZFS terms has been attempted[4] (cf. also Ref. 5, Chap. IV B 1) using the transformation matrices $S_k(\Phi,\Theta)$ for the Stevens operators[6] and the algebraic program ALTRAN.[7] Further considerations have, however, revealed that the model[1] has only an *ad hoc* justification. Instead, a *net charge-compensation* (NCC) model, which correlates in a symmetry-consistent way the fine structure for a charge-compensated EPR defect center with that for a nonlocally compensated one, has been proposed.[8] The NCC model[8] comprises the previous one[1] as a special case. The NCC model has been applied[8] to M'^{3+}-V_M (cation vacancy) and M'^{3+}-A'^{+} (M' represents Cr, Fe, and Gd; A' represents Li and Na) centers in A_2MF_4 (Refs. 1-3) and A_2MCl_4.[9] In this paper the EPR data on several defect centers, namely Cr^{3+}, Fe^{3+}, and Gd^{3+} in A_2MF_4-, A_2MCl_4-, AMF_3-, MF_2-, and MCl_2-type crystals, are analyzed in terms of the net charge-compensation model. Relationships between the NCC model[8] and the description[10,11] of the EPR results for Gd^{3+} in MX_2 crystals as well as the models[12] of the crystal field for Yb^{3+} in CaF_2 are also discussed. Other possible applications of the NCC model are suggested.

II. OUTLINE OF THE MODEL

Since a detailed derivation of the net charge-compensation model is given elsewhere,[8] we quote here only the final result. The considerations[8] are based on the superposition idea originally developed for the crystal-field Hamiltonian[13] and later extended for the spin Hamiltonian.[14] [Note the relationships[15] between the superposition model formulas[13,14] and the transformation matrices $S_k(\Phi,\Theta)$ for the Stevens operators.[6]] We denote the experimentally observed ZFS Hamiltonian for a charge-compensated (CC) EPR center by $\mathcal{H}_{\text{expt}}$ and that for an otherwise undistorted (und) vacancy center in the same crystal by $\mathcal{H}_{\text{expt}}^{\text{und}}$. The symmetry of $\mathcal{H}_{\text{expt}}$, given by a point group G, is lower than that of $\mathcal{H}_{\text{expt}}^{\text{und}}$, i.e., G_0, due to the presence of the charge compensator in the nearest (NN) or next-nearest (NNN) neighborhood of the CC EPR center. A vacancy or a

charge-compensating ion is likely to introduce distortions of the NN ligands, further lowering the symmetry around the CC EPR center. The NCC model relates the two Hamiltonians as follows:

$$\mathcal{H}_{\text{expt}}(G)=\mathcal{H}^{\text{und}}_{\text{expt}}(G_0)+\mathcal{H}_{\text{CC}}(G') \tag{1}$$

or, explicitly in terms of the Stevens operators,[6]

$$\sum_{k,q} B^q_k O^q_k=\sum_{k,q} B^q_k(\text{und})\{O^q_k\}+\sum_{k,q} B'^q_k\{O^q_k\}' , \tag{2}$$

where the curly brackets denote the operators in the original[6,16] (local) axis system. The term $\mathcal{H}_{\text{CC}}$ in (1) and (2) represents the *net charge-compensation* contribution to the fine structure of the CC EPR defect center. A general restriction on $\mathcal{H}_{\text{CC}}$ is that $\mathcal{H}_{\text{CC}}$ must be of a symmetry G' (to be established) which does not lead to $\mathcal{H}_{\text{expt}}$ on the left-hand side (lhs) of Eq. (1) of symmetry lower than actually observed. The net charge-compensation contribution parameters B'^q_k can then be expressed in terms of B^q_k and B^q_k(und) known from experiment. The transformation matrices[6] $S_k(\Phi,\Theta)$ and/or the relations between the parameters B^q_k in various axis systems[16] are then very useful.

For example, in the case of the Cr^{3+} centers III and IV associated with a vacancy at the nearest divalent cation site and an A'^{+} ion (A' represents Na and Li), respectively, in A_2MF_4 (Refs. 1–3) or A_2MCl_4,[9] $\mathcal{H}_{\text{expt}}$ is orthorhombic and $\mathcal{H}^{\text{und}}_{\text{expt}}$ (center I) is tetragonal. It has been shown[8] that the model of Takeuchi *et al.*[1] for Cr^{3+} ($S=\frac{3}{2}$) corresponds to the choice $\mathcal{H}_{\text{CC}}$(axial) in Eq. (1). However, the most general form of $\mathcal{H}_{\text{CC}}$ for centers III and IV in these crystals is orthorhombic with the principal axis taken along the vacancy (or A'^{+} ion) axis. Numerical results[8] indicate the orthorhombic component induced by charge compensation (B'^2_2) is significant for these centers and hence the approximation[1-3] $B'^2_2\equiv 0$ is not justified. Analysis for the M'^{3+} centers II in A_2MF_4 (Ref. 1) and A_2MCl_4 (Ref. 9) associated with a vacancy at the nearest A^{+} site is more complex and is presented below.

III. Cr^{3+}, Fe^{3+}, AND Gd^{3+} TYPE-II CENTERS IN A_2MF_4 AND A_2MCl_4 CRYSTALS

The immediate neighborhood of center II in A_2MX_4 crystals is depicted in Fig. 1. Takeuchi *et al.*[1] considered the superposition of $D_1S^2_{z'}$ and $D_2S^2_{z''}$, which yields an orthorhombic ZFS Hamiltonian in a special axis system with the angle φ given by the relation $D_1/D_2=\sin(2\phi)/\sin(2\varphi)$. Their x and y axes are along the $-y$ and $+x$ axes in Fig. 1, respectively. The symmetry of the site is monoclinic with the monoclinic axis along the y axis in Fig. 1. There are three choices of the monoclinic axis C_2 possible;[17] one[1] corresponds to $x\|C_2$ and yields the monoclinic term $B^{-1}_2O^{-1}_2$, whereas our choice corresponds to $y\|C_2$ and yields the monoclinic term $B^1_2O^1_2$. The latter choice is more convenient and has also been used[9] for Cr^{3+} in Cs_2CdCl_4. This choice corresponds to the trigonal axis system with $x''\|[11\bar{2}]$ and $y''\|[\bar{1}10]$ being adopted for the $D_2S^2_{z''}$ term. The

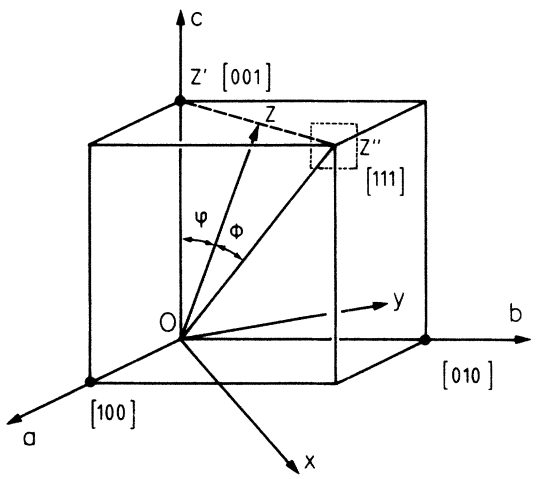

FIG. 1. The axis system for the A^{+}-vacancy-associated Cr^{3+} center II in A_2MX_4 crystals.

choice of Takeuchi *et al.*[1] corresponds to adopting the trigonal axis system with $x''\|[1\bar{1}0]$ and $y''\|[11\bar{2}]$. The two axis systems have been denoted[16,5] "Watanabe" and "Orton," respectively. The third possible trigonal axis system is that of "Hutchings" ($x''\|[\bar{1}\bar{1}2]$, $y''[1\bar{1}0]$)—for detailed references, see Refs. 16 and 5.

The NCC model, Eq. (2), yields for center II the following second-order equation:

$$B^0_2O^0_2+B^2_2O^2_2+B^1_2O^1_2=B^0_2(I)\{O^0_2\}+B'^0_2\{O^0_2\}'+B'^2_2\{O^2_2\}'+B'^1_2\{O^1_2\}' , \tag{3}$$

where the operators O^q_k, $\{O^q_k\}$, and $\{O^q_k\}'$ are expressed in the axis systems (x,y,z), $(x'\|a, y'\|b, z'\|c)$, and $(x''\|[11\bar{2}]$, $y''\|[\bar{1}10]$, $z''\|[111])$, respectively. The monoclinic parameter B^1_2 can be set to zero by a rotation $\alpha/0y$ with the angle α given by[17]

$$\tan(2\alpha)=B^1_2/(3B^0_2-B^2_2) . \tag{4}$$

Since the experimental values[1,9] of $D(\sim B^0_2)$ and $E(\sim B^2_2)$ are given in this special axis system, i.e., with $B^1_2=0$ (Ref. 9) [$B^{-1}_2=0$ (Ref. 1)] and $\varphi=\alpha$, it is most convenient to adopt this system for the ZFS term on the lhs of Eq. (3). On the other hand, an arbitrary rotation around the monoclinic axis leaves the form of $\mathcal{H}_{\text{CC}}$ in (3) invariant with the parameters B'^0_2, B'^2_2, and B'^1_2 modified.[15] Hence transformation of $\mathcal{H}_{\text{expt}}$ and $\mathcal{H}_{\text{CC}}$ in (3) to this axis system yields

$$[B^0_2][O^0_2]+[B^2_2][O^2_2]=B^0_2(I)\{O^0_2\}+[B'^0_2][O^0_2]+[B'^2_2][O^2_2]+[B'^1_2][O^1_2] , \tag{5}$$

where the square brackets indicate that the parameters and operators are now expressed in the special axis system. Using the transformation (45°,0°) followed by a rotation by α around the new y' axis,[16] we obtain the following relations:

$$[B_2'^2]=[B_2^2]-\tfrac{3}{2}(\sin^2\alpha)B_2^0(I)\ ,$$
$$[B_2'^1]=3\sin(2\alpha)B_2^0(I)\ , \tag{6}$$
$$[B_2'^0]=[B_2^0]-\tfrac{1}{2}(3\cos^2\alpha-1)B_2^0(I)\ .$$

Numerical results are given in Table I using $[b_2^0]=D$ and $[b_2^2]=-3E$ of Ref. 1 [the minus sign arises because the (x,y,z) system[1] is rotated by $(\pm 90°,0°)$ with respect to the (x,y,z) system in Fig. 1] and $[b_2^2]=3E$ of Ref. 9. The procedure of Takeuchi *et al.*[1] corresponds to setting $B_2'^2=B_2'^1\equiv 0$ in (3) and results in a different set of equations. In order to enable direct comparison between their results and ours, the parameters $b_2'^q$ in the axis system (x'',y'',z'') obtained by a rotation $\phi=54.73°-\alpha$ around the y axis[16] are also given in Table I. For example, for the Cr^{3+} center II in K_2ZnF_4 at 77 K the authors[1] adopt $D_2(=b_2'^0)=-1613\times10^{-4}$ cm^{-1} taken from the trigonal center in $KZnF_3$, as compared with the value -1849.7×10^{-4} cm^{-1} derived in Table I without the implausible[8] resort to data on AMF_3. The values of $b_2'^1$ in Table I indicate the approximation[1] $b_2'^1\equiv 0$ is hardly justified for the Cr^{3+} centers II in all A_2MX_4 crystals studied. Moreover, the neglect[1] of $b_2'^2$ for the Cr^{3+} centers II in all K_2MgF_4 and Cs_2CdCl_4 appears also not justified.

Extension of the NCC model for the higher-spin EPR centers II in A_2MX_4 leads to the following equations [in the notation used in Eq. (5)]:

$$\sum_{q=1}^{4}[B_4^q][O_4^q]=B_4^0(I)\{O_4^0\}+B_4^4(I)\{O_4^4\}+\sum_{q=1}^{4}[B_4'^q][O_4^q] \tag{7}$$

and

$$\sum_{q=1}^{6}[B_6^q][O_6^q]=B_6^0(I)\{O_6^0\}+B_6^4(I)\{O_6^4\}+\sum_{q=1}^{6}[B_6'^q][O_6^q]\ . \tag{8}$$

Solving Eqs. (7) and (8) in the same way as in the derivation of Eq. (6), we obtain the relations

$$[B_4'^4]=[B_4^4]+B_4^4(I)\tfrac{1}{8}(\cos^4\varphi+6\cos^2\varphi+1)-B_4^0(I)\tfrac{35}{8}\sin^4\varphi\ ,$$
$$[B_4'^3]=[B_4^3]+B_4^4(I)\sin\varphi\cos\varphi(\cos^2\varphi+3)+B_4^0(I)35\sin^3\varphi\cos\varphi\ ,$$
$$[B_4'^2]=[B_4^2]+B_4^4(I)\tfrac{1}{2}\sin^2\varphi(\cos^2\varphi+1)-B_4^0(I)\tfrac{5}{2}\sin^2\varphi(7\cos^2\varphi-1)\ , \tag{9}$$
$$[B_4'^1]=[B_4^1]+B_4^4(I)\sin^3\varphi\cos\varphi+B_4^0(I)5\sin\varphi\cos\varphi(7\cos^2\varphi-3)\ ,$$
$$[B_4'^0]=[B_4^0]+\tfrac{1}{8}B_4^4(I)\sin^4\varphi-B_4^0(I)\tfrac{1}{8}(35\cos^4\varphi-30\cos^2\varphi+3)\ ,$$

and

$$[B_6'^6]=[B_6^6]+B_6^4(I)\tfrac{11}{32}\sin^2\varphi(\cos^4\varphi+6\cos^2\varphi+1)-B_6^0(I)\tfrac{231}{32}\sin^6\varphi\ ,$$
$$[B_6'^5]=[B_6^5]+B_6^4(I)\tfrac{11}{8}\sin\varphi\cos\varphi(3\cos^4\varphi+10\cos^2\varphi-5)+B_6^0(I)\tfrac{693}{8}\sin^5\varphi\cos\varphi\ ,$$
$$[B_6'^4]=[B_6^4]+B_6^4(I)\tfrac{1}{16}(33\cos^6\varphi+35\cos^4\varphi-65\cos^2\varphi+13)-B_6^0(I)\tfrac{63}{16}\sin^4\varphi(11\cos^2\varphi-1)\ ,$$
$$[B_6'^3]=[B_6^3]+B_6^4(I)\tfrac{5}{8}\sin\varphi\cos\varphi(11\cos^4\varphi+2\cos^2\varphi-5)+B_6^0(I)\tfrac{105}{8}\sin^3\varphi\cos\varphi(11\cos^2\varphi-3)\ ,$$
$$[B_6'^2]=[B_6^2]+B_6^4(I)\tfrac{5}{32}\sin^2\varphi(33\cos^4\varphi-10\cos^2\varphi+1)-B_6^0(I)\tfrac{105}{32}\sin^2\varphi(33\cos^4\varphi-18\cos^2\varphi+1)\ , \tag{10}$$
$$[B_6'^1]=[B_6^1]+B_6^4(I)\tfrac{1}{4}\sin^3\varphi\cos\varphi(33\cos^2\varphi-13)+B_6^0(I)\tfrac{21}{4}\sin\varphi\cos\varphi(33\cos^4\varphi-30\cos^2\varphi+5)\ ,$$
$$[B_6'^0]=[B_6^0]+B_6^4(I)\tfrac{1}{16}\sin^4\varphi(11\cos^2\varphi-1)-B_6^0(I)\tfrac{1}{16}(231\cos^6\varphi-315\cos^4\varphi+105\cos^2\varphi-5)\ .$$

TABLE I. Zero-field-splitting parameters for the Cr^{3+} type-II centers in A_2MX_4 crystals (all in 10^{-4} cm^{-1}). Experimental values of $b_2^0(I)$, $[b_2^0]$, $[b_2^2]$, and α are taken from references as indicated. The primed parameters $[b_2'^q]$ and $b_2'^q$ derived here describe the net effect of charge compensation in the special axis system with $[b_2^1]=0$ and the trigonal axis system, respectively. RT denotes room temperature.

	T (K)	$b_2^0(I)$	$[b_2^0]$	$[b_2^2]$	α (deg)	$[b_2'^0]$	$[b_2'^1]$	$[b_2'^2]$	$b_2'^0$	$b_2'^1$	$b_2'^2$
K_2ZnF_4[a]	293	−381	−1872	−288	44.0	−1766.8	−1142.3	−12.2	−1779.6	872.6	0.6
	77	−374	−1937	−279	44.5	−1838.6	−1121.8	−3.4	−1849.7	876.9	7.7
	4.2	−376	−1948	−279	44.1	−1845.1	−1127.4	−5.9	−1853.2	955.4	2.2
K_2MgF_4[a]	293	−419	−1861	−141	43.1	−1735.4	−1254.2	+152.4	−1750.3	964.9	167.3
Cs_2CdCl_4[b]	RT?	±228	∓758	±108	∼35	∓873.5	±642.8	∓4.5	∓622.2	±2159.1	∓255.8
		±228	±758	∓108	∼35	±642.5	±642.8	∓220.5	±622.2	∓869.3	∓200.2

[a]Reference 1.
[b]Reference 9.

Analysis of the net charge-compensation contributions $[B_4'^q]$ and $[B_6'^q]$ is not possible at present because of lack of relevant EPR data on M'^{3+} ($S \geq 2$) centers II in A_2MX_4. The results on Fe^{3+} in K_2ZnF_4 are expected to become available in the near future.[18]

IV. Cr^{3+}, Fe^{3+}, and Gd^{3+} CENTERS IN AMF_3 CRYSTALS

EPR studies[19–24] on the Cr^{3+} ions in AMF_3 perovskite fluorides reveal the centers analogous to the Cr^{3+} centers[1–3] I–IV in A_2MF_4. Temperature dependence of the EPR spectrum provides useful information on the structural phase transitions in $KCdF_3$ (Ref. 23) and $RbCdF_3$ (Refs. 25 and 26). However, since the symmetry of the nonlocally charge-compensated Cr^{3+} centers I in the cubic phase AMF_3 studied so far[22] is cubic (and hence no ZFS is observed), the experimentally observed axial parameter D ($=b_2^0$) for the charge-compensated centers II (trigonal), III, and IV (both tetragonal) is entirely due to the charge compensation, i.e., $b_2'^0 \equiv b_2^0$.

Two types of the vacancy associated Fe^{3+} centers in AMF_3 have been observed: *trigonal*—due to an A^+ vacancy along a ⟨111⟩ axis in $KZnF_3$ (Ref. 27) and $KMgF_3$ (Ref. 28), and *tetragonal*—due to an M^{2+} vacancy along a ⟨100⟩ axis in $KZnF_3$,[19] $RbCdF_3$, and $CsCdF_3$.[20] The cubic parameter a_c for the vacancy-free Fe^{3+} center has been reported for several AMF_3 crystals.[29–33] The Fe^{3+} ion has been used as a probe in EPR and electron-nuclear double-resonance (ENDOR) studies of the structural phase transitions in $RbCaF_3$ (Ref. 34) and $RbCdF_3$ (Ref. 35), respectively. The NCC model, Eq. (2), yields for the trigonal centers the fourth-order equation

$$B_4^0 O_4^0 + B_4^3 O_4^3 = B_4(\{O_4^0\} + 5\{O_4^4\}) + B_4'^0 O_4^0 + B_4'^3 O_4^3 , \tag{11}$$

where $B_4 = B_4^0(I)$ and the operators O_4^q are expressed in one of the three trigonal axis systems[5,16] (see Sec. III), and $\{O_4^q\}$ are referred to the cubic axis. Hence, the relations follow

$$\begin{aligned} B_4'^0 &= B_4^0 + \tfrac{2}{3}B_4 , \\ B_4'^3 &= B_4^3 \pm (40\sqrt{2}/3)B_4 , \end{aligned} \tag{12}$$

where the upper and lower signs refer to the Watanabe and Hutchings systems, respectively. The relations (12) also apply for the parameters b_4^q, provided consistent scaling[14,5] is used (then $b_4 = a_c/2$). The authors[27,28] use the Hutchings axis system. Using the relations[5] for conversion of the conventional parameters[27] a and F to $B_4^q(b_4^q)$, we obtain the same results as quoted in Ref. 28. The corresponding net charge-compensation contributions are listed in Table II. (Note that for Fe^{3+} at cubic sites in $KMgF_3$ there is a disagreement concerning the value a_c at 300 K in Refs. 29 and 28. We believe the value $|a_c| = 6.5 \times 10^{-4}$ cm^{-1} of Ref. 29 is, instead, a misprint—cf. also Ref. 32.) For the tetragonal Fe^{3+} centers in AMF_3 (Refs. 19 and 20) we have Eq. (11) with $q=3$ replaced by $q=4$ and all the operators expressed in the cubic axis. Hence the relations are straightforward:

$$B_4'^0 = B_4^0 - B_4 , \quad B_4'^4 = B_4^4 - 5B_4 , \tag{13}$$

and using the conversion relations[5] we obtain

$$b_4'^0 = \tfrac{1}{2}(a - a_c) + F/3 , \quad b_4'^4 = \tfrac{5}{2}(a - a_c) . \tag{14}$$

The corresponding numerical results are also included in Table II. Tetragonal Fe^{3+} centers have also been observed[20] in $CsCdF_3$; however, no data on a_c have been found in the literature for this case (cf. e.g., Ref. 32). The Stevens operator notation enables, unlike the conventional notation, direct conclusions on the relative size of the charge-compensation contributions to the fine structure of the defect centers. Table II reveals that an approximation of the net charge-compensation contribution $\mathcal{H}_{CC}$ in Eq. (2) by a uniaxial term $b_4'^0 O_4'^0$, which follows from a straightforward extension of the model,[1] would be highly inappropriate for the trigonal and tetragonal Fe^{3+} centers in AMF_3 crystals.

There exists another type of strongly tetragonal Fe^{3+} defect center in AMF_3 crystals which is associated with an O^{2-} ion substituted for a NN fluorine.[35–38] The fourth-order ZFS parameters for this ($FeOF_5$) cluster center at room temperature have been determined for Fe^{3+} in $KZnF_3$ partially as $a=25$ with F neglected[36] and for Fe^{3+} in $KMgF_3$ as $b_4^0 = +75$ and $b_4^4 = +269$ with $b_2^0 = -3572$ (in 10^{-4} cm^{-1}).[38] The latter b_4^q values yield, using Eq. (13), which applies to this center too, the net charge-compensation contributions as $b_4'^0 = 49.4$ and $b_4'^4 = 141$ (10^{-4} cm^{-1}). Comparing these values with

TABLE II. The net charge-compensation contributions $b_k'^q$ derived from the experimental data for Fe^{3+} at the vacancy-associated trigonal and tetragonal sites in perovskite fluorides at $T=300$ K (in 10^{-4} cm^{-1}).

	Trigonal sites				Tetragonal sites			
	$KZnF_3$	Ref.	$KMgF_3$	Ref.	$KZnF_3$	Ref.	$RbCdF_3$	Ref.
$b_4 = a_c/2$	+26.4	30	+25.6	28	+26.4	30	+22.3	31
$b_2'^0 = b_2^0$	+103.4	27	+87.2	28	−759.0	20	−422.2	20
b_4^0	−16.5	27	−13.7	28	+29.8	20	+24.9	20
$b_4^3(b_4^4)$	+429.9	27	+356.0	28	(+97.5)	20	(+93.3)	20
$b_4'^0$	+1.07	a	+3.37	a	+3.5	a	+2.7	a
$b_4'^3(b_4'^4)$	−67.0	a	−126.7	a	(−34.3)	a	(−18.0)	a

[a]This work.

those in Table II for the vacancy-associated Fe^{3+} centers in AMF_3, one notes a much higher NCC contribution to $B_4'^0$ as well as a higher contribution (with opposite sign) to $b_4'^4$ in the former case.

The Gd^{3+}-V_M centers[39–45] and Gd^{3+}-O^{2-} centers[40,42,46–48] analogous to the two types of tetragonal Fe^{3+} centers discussed above are observed only in the cubic phase $ACaF_3$ and $ACdF_3$, where the Gd^{3+} ion enters the M^{2+} octahedral site. In AMF_3 hosts with smaller M^{2+} ions (Zn^{2+}, Mg^{2+}) the Gd^{3+} ion substitutes for the alkaline-earth A^+ ion at a 12-coordinated site (cf. e.g., Refs. 42 and 49). These tetragonal Gd^{3+} centers provide[40–43,46,47] a sensitive EPR probe for studying the structural phase transitions[48] in $RbCdF_3$ and $RbCaF_3$. Application of the NCC model for these studies has to be deferred to a separate paper. Recently also the Gd^{3+}-Li^+ centers have been observed[45] in the cubic-phase $ACaF_3$ and $ACdF_3$. These centers exhibit the same tetragonal symmetry as the Gd^{3+}-V_M centers.[45] The NCC model, Eq. (2), yields for the three types of tetragonal centers the sixth-order equation (in the cubic axis system)

$$B_6^0 O_6^0 + B_6^4 O_6^4 = B_6(O_6^0 - 21O_6^4) + B_6'^0 O_6^0 + B_6'^4 O_6^4 , \quad (15)$$

and hence the relations

$$\begin{aligned} B_6'^0 &= B_6^0 - B_6 , \\ B_6'^4 &= B_6^4 + 21B_6 . \end{aligned} \quad (16)$$

Among the pertinent EPR studies,[39–45] the most extensive one, combining the investigations of the Gd^{3+}-V_M and Gd-Li^+ centers, are those of Arakawa *et al.*[45] Using Eqs. (13) and (16) the net charge-compensation contributions $b_k'^q$ are derived and listed in Table III for the two types of Gd^{3+} centers in several AMF_3 hosts. In order to reduce the size of this tabulation the original values of the tetragonal b_k^q and cubic b_k parameters are not given here but only the original source reference is indicated. Table III provides information on the temperature variation of the parameters $b_k'^q$ for some AMF_3 hosts. Comparison of Table II with Tables I and II of Ref. 45 and Table I of Ref. 44 reveals the following. The $b_4'^0$ contribution to b_4^0 is substantial and of opposite sign to that of the cubic b_4, whereas the $b_4'^4$ contribution to b_4^4 is substantial and of the same sign as the cubic cubic contribution ($5b_4$) for both Gd^{3+} centers in all AMF_3 hosts studied. The $b_6'^0$ contribution to b_6^0 is rather small in all the hosts and changes sign with temperature for $RbCdF_3$ and $CsCdF_3$. The $b_6'^4$ contribution is also small in all the hosts, except $KCdF_3$, and no uniform sign behavior is observed. An approximation of the charge-compensation contribution by a uniaxial term for both the fourth- and sixth-order ZFS terms would fail for the Gd^{3+}-V_M and Gd^{3+}-Li^+ centers in AMF_3.

The EPR data on the Gd^{3+}-O^{2-} centers in AMF_3 are rather patchy. For illustration, using the tetragonal $b_4^0 = 2$, $b_4^4 = -100$, $b_6^0 = -3$, $b_6^4 \sim 0$ and the cubic $b_4 = -4.92$, $b_6 = +0.83$ for the Gd^{3+}-O^{2-} center[42] in $RbCaF_3$ at 300 K, we obtain $b_4'^0 = 6.92$, $b_4'^4 = -75.4$, $b_6'^0 = -3.83$, and $b_6'^4 = +17.4$ (all in 10^{-4} cm^{-1}). The conclusions on the $b_4'^q$ contributions for the Gd^{3+}-V_M and Gd^{3+}-Li^+ centers hold also for this Gd^{3+}-O^{2-} center, while the experimental accuracy[42] of the parameters b_6^0 and b_6^4 does not warrant any definite conclusion in the present case.

Although, to the best of our knowledge, no trigonal Gd^{3+} centers have been observed in AMF_3 crystals, for possible future use we give here the corresponding expressions for this case also:

$$\begin{aligned} B_6'^0 &= B_6^0 - \tfrac{16}{9}B_6 \\ B_6'^3 &= B_6^3 \pm (140\sqrt{2}/9)B_6 \\ B_6'^6 &= B_6^6 - \tfrac{154}{9}B_6 , \end{aligned} \quad (17)$$

where the same notation as in Eqs. (11) and (12) is used.

V. ORTHORHOMBIC Gd^{3+} CENTERS IN MX_2 CRYSTALS

EPR studies of Gd^{3+} in the alkaline-earth halides CdF_2,[50] CaF_2,[51,10,11,53] BaF_2,[11] $SrCl_2$,[52] and SrF_2 (Ref. 54) reveal orthorhombic centers due to the Gd^{3+}-A'^+ (A' represents Li–Ca) complexes. Two axis systems

TABLE III. The net charge-compensation contributions $b_k'^q$ derived from the experimental data taken from the references as indicated, for the tetragonal Gd^{3+} centers in AMF_3 (in 10^{-4} cm^{-1}).

		Reference		Gd^{3+}-V_M center				Gd^{3+}-Li^+ centers			
Host	T (K)	b_k^q	b_k	$b_4'^0$	$b_4'^4$	$b_6'^0$	$b_6'^4$	$b_4'^0$	$b_4'^4$	$b_6'^0$	$b_6'^4$
$KCdF_3$	487	45	44,49	+1.30	−17.9	−0.20	+6.30	+1.09	−15.0	−0.10	+5.30
$RbCdF_3$	487	45	44	+2.19	−18.9	+0.05	−2.67	+2.12	−17.3	−0.04	−2.67
	302 (300)	45	(42)	+2.28	−19.6	−0.04	−1.05	+2.00	−16.3	+0.01	+0.65
$RbCaF_3$	297 (300)	45	(42)	+2.06	−18.3	+0.00	−0.07	+1.96	−19.4	+0.03	−1.77
$CsCdF_3$	487	45	44	+2.13	−22.5	+0.04	−2.04	+2.25	−22.9	−0.01	−0.54
	300 (296)	45	(44)	+2.44	−22.3	−0.05	−0.84	+2.56	−22.9	−0.04	−0.94
$CsCaF_3$	487	45	44	+2.42	−22.1	−0.17	+1.06	+2.63	−26.2	+0.03	−0.94
	298 (296)	45	(44)	+2.44	−22.4	−0.07	−0.31	+2.78	−27.0	−0.04	+0.29

with the z axis along the Gd^{3+}-A'^{+} direction have been adopted for these centers: (i) with the y axis[50,51,10] and (ii) with the x axis[11,52–54] being parallel to the cube edge perpendicular to the z axis. The two systems are related by a $\pm 90°/0z$ rotation and hence the signs of B_k^2 and B_6^6 are reversed. The fourth- and sixth-order NCC model equations are then

$$\sum_q B_4^q O_4^q = B_4(\{O_4^0\} + 5\{O_4^4\}) + \sum_q B_4'^q O_4^q \tag{18}$$

and

$$\sum_q B_6^q O_6^q = B_6(\{O_6^0\} - 21\{O_6^4\}) + \sum_q B_6'^q O_6^q \ . \tag{19}$$

Upon transforming the cubic term, as is appropriate for the two systems, we obtain

$$\begin{aligned} B_4'^0 &= B_4^0 + \tfrac{1}{4}B_4 \ , \\ B_4'^2 &= B_4^2 \mp 5B_4 \ , \\ B_4'^4 &= B_4^4 - \tfrac{15}{4}B_4 \ , \end{aligned} \tag{20}$$

and

$$\begin{aligned} B_6'^0 &= B_6^0 - \tfrac{13}{8}B_6 \ , \\ B_6'^2 &= B_6^2 \pm \tfrac{105}{16}B_6 \ , \\ B_6'^4 &= B_6^4 + \tfrac{105}{8}B_6 \ , \\ B_6'^6 &= B_6^6 \pm \tfrac{231}{16}B_6 \ , \end{aligned} \tag{21}$$

where the upper and lower signs refer to the above defined (i) (Refs. 50, 51, and 10) and (ii) (Refs. 11, and 52–54) axis systems, respectively.

The early experimental data[50] for Gd^{3+} in GdF_2 were given in the mixed-axis system notations (for details, see the review[5]) with the fourth-order ZFS term truncated to a cubiclike term only. That enabled a direct, although approximate, comparison of the cubic B_4 and the noncubic B_4 parameters.[50] The authors[10] measured all b_k^q, $k=2$, 4, and 6, for the Gd^{3+}-Na^+ centers in CaF_2. Additionally they gave their fourth-order results in terms of the "parameter shifts," i.e., the differences between the rhombic and cubic parameters (referred to the same axis system[5]). This approach is thus an example of an implicit use of the NCC model as given by the relations (20). The approach[10] has later been used by Bijvank *et al.*,[11] although in both cases[10,11] no explicit relations were given and the discussion[11] of the parameter shifts was again limited to the fourth-order parameters. An extension of the NCC model analysis to the sixth-order ZFS terms is possible for the data,[10] while the data[11] comprise only B_6^0. Using the values[10] $b_6^0 = 1.4$, $b_6^2 = 7.4$, $b_6^4 = 0.7$, $b_6^6 = 15.8$, and the value[55,56] $b_6 = (\frac{1}{4}d)$ (Ref. 57) $= 1$ (in 10^{-4} cm^{-1}), we obtain, from (21), the sixth-order net charge-compensation contributions for the Gd^{3+}-Na^+ centers in CaF_2 at room temperature as $b_6'^0 = -0.23$, $b_6'^2 = 14.0$, $b_6'^4 = 13.8$, and $b_6'^6 = 30.2$ (in 10^{-4} cm^{-1}). This analysis shows the significance of the $b_6'^2$, $b_6'^4$, and $b_6'^6$ contributions for the present case. Caution is, however, necessary since Table II of the review[58] indicates the values of b_6 for Gd^{3+} in MX_2 crystals vary with dilution. No more pertinent data on Gd^{3+} in MX_2, particularly in CaF_2, than those already discussed here are listed in the recent review.[59] Hence, a more detailed analysis of the NCC model parameters $b_6'^q$ for the orthorhombic Gd^{3+} centers in alkaline-earth halides must await more accurate measurements of b_6^q and b_6.

The second-order ZFS parameters b_2^0 and b_2^2 are wholly due to the charge compensation for the Gd^{3+}-M^+ centers in MX_2 crystals. In the axis systems (i) and/or (ii), for some centers, the ratio $\lambda = b_2^2/b_2^0$ appears to be in the nonstandard range (for definitions, see Ref. 60). Application of the standardization of the parameters b_k^q for these cases has already been discussed.[5,60] The standardization[60] may be helpful for comparison of the nonstandard results with those standardized.[5]

VI. DISCUSSION

The above applications of the net charge-compensation model indicate its usefulness, especially for paramagnetic centers at *low*-symmetry sites involving a charge-compensation mechanism. The NCC model provides a clear relationship, based on symmetry, between the ZFS Hamiltonian for the undistorted (i.e., remotely compensated) centers and that for the distorted (i.e., locally compensated centers). The relations derived here enable determination of the net contributions to ZFS parameters due to the charge compensation. The NCC model turns out to be more general than the superposition of two uniaxial ZFS terms proposed by Takeuchi *et al.*[1] for the Cr^{3+} centers in A_2MX_4 crystals. Moreover, the present model is applicable to any order ZFS terms. The previous model[1] has been applied only to the second-order ZFS terms.[1–3] Our preliminary calculations[4] have shown that not all the model parameters could be extracted from the equations resulting from a straightforward extension of the model[1] to the fourth- and sixth-order ZFS terms.

The NCC model has been applied to the trivalent EPR defect centers in A_2MX_4 (cf. also Ref. 8), AMX_3-, and MX_2-type crystals. Interestingly, the model is found to have earlier been implicitly used[10,11] for the Gd^{3+}-M^+ centers in MX_2 crystals. A survey of the literature reveals other possible applications of the NCC model. The orthorhombic and axial Mn^{2+} centers in alkali halides have been extensively studied by EPR (cf. e.g., Refs. 61–67, and references therein). However, the isolated Mn^{2+} (cubic) centers have been observed only in NaCl at room temperature and the available cubic parameter a is rather tentative.[68] EPR studies of the orthorhombic Eu^{2+} centers in alkali halides are also extensive (cf. e.g., Refs. 69–76, and references therein), whereas the data on the cubic Eu^{2+} centers concern NaCl (Ref. 77) and KCl (Ref. 78) at room temperature only. The trivalent impurities, like Cr^{3+} and Fe^{3+}, in MgO (Refs. 79–82) and $SrTiO_3$ (Refs. 81–84), and the related crystals may serve as other possible systems for the NCC model studies. The EPR centers are known as good probes for studying structural phase transitions.[85]

Although the applications of the NCC model con-

sidered here concern the spin-Hamiltonian analysis, similar applications to the crystal-field analysis seem feasible. Hence it is worthwhile to consider the relationship between the NCC model and the models of the crystal field for a trigonal Yb^{3+} site in CaF_2 discussed by Baker and Davies.[12] The three models are described by the following Hamiltonians:

$$\mathcal{H}_T=\mathcal{H}_c+A_2^0O_2^0 \quad \text{(model I)},$$

$$\mathcal{H}_T=\mathcal{H}_c+A_2^0O_2^0+A_4^0O_4^0+A_6^0O_6^0 \quad \text{(model II)},$$

$$\mathcal{H}_T=\tau\mathcal{H}_c+A_2^0O_2^0+A_4^0O_4^0+A_6^0O_6^0 \quad \text{(model III)},$$

where $\mathcal{H}_c$ is the crystal field of the cubic site and τ is a scaling parameter. (For references on the use of each of the models see Ref. 12.) From the point of view of the NCC model, applied to the crystal-field Hamiltonian for this particular case, the most general form of the trigonal $\mathcal{H}_T=\mathcal{H}_c+\mathcal{H}(\mathrm{CC})$ requires the net charge-compensation contribution $\mathcal{H}(\mathrm{CC})$ to be of the same form as $\mathcal{H}_T$, Eq. (2) in Ref. 12, in a given trigonal axis system, i.e.,

$$\mathcal{H}(\mathrm{CC})=A_2^0O_2^0+A_4^0O_4^0+A_4^3O_4^3+A_6^0O_6^0+A_6^3O_6^3+A_6^6O_6^6 .$$

Hence it turns out that the first two models[12] are subsequent approximations to the most general NCC model,[8] while model III is rather unphysical since it assumes a modified cubic crystal field.

Finally, we note that in several papers discussed here the ZFS parameters are inappropriately called the crystal-field parameters. This contributes to the confusion between the spin Hamiltonian and the crystal-field Hamiltonian, which has been discussed at length in the recent review.[5]

ACKNOWLEDGMENTS

The author would like to thank Dr. R. Bramley for helpful discussions and a critical reading of the manuscript. Helpful correspondence with Dr. M. Arakawa and Dr. H. Takeuchi is gratefully acknowledged.

[1]H. Takeuchi, M. Arakawa, H. Aoki, T. Yosida, and K. Horai, J. Phys. Soc. Jpn. **51**, 3166 (1982).
[2]H. Takeuchi and M. Arakawa, J. Phys. Soc. Jpn. **52**, 279 (1983).
[3]M. Arakwa, H. Ebisu, and H. Takeuchi, J. Phys. Soc. Jpn. **55**, 2853 (1986).
[4]C. Rudowicz, in Conference Handbook—11th Condensed Matter Physics Meeting, Pakatoa Island, New Zealand, 1987.
[5]C. Rudowicz, Magn. Res. Rev. **13**, 1-89 (1987).
[6]C. Rudowicz, J. Phys. C **18**, 1415 (1985).
[7]C. Rudowicz, Aust. Phys. **21**, 275 (1984), and references therein.
[8]C. Rudowicz, Solid State Commun. (to be published).
[9]D. Kay and G. L. McPherson, J. Phys. C **14**, 3247 (1981).
[10]A. Edgar and D. J. Newman, J. Phys. C **8**, 4023 (1975).
[11]E. J. Bijvank, H. W. den Hartog, and J. Andriessen, Phys. Rev. B **16**, 1008 (1977).
[12]J. M. Baker and E. R. Davies, J. Phys. C **8**, 1869 (1975).
[13]See, D. J. Newman, Adv. Phys. **20**, 197 (1971), and references therein.
[14]See, D. J. Newman and W. Urban, Adv. Phys. **24**, 793 (1975), and references therein.
[15]C. Rudowicz, J. Phys. C (to be published).
[16]C. Rudowicz, J. Magn. Res. **63**, 95 (1985).
[17]C. Rudowicz, J. Chem. Phys. **84**, 5045 (1986).
[18]H. Takeuchi (private communication).
[19]M. Binois, A. Leble, J. J. Rousseau, and J. C. Fayet, J. Phys. (Paris) Colloq. **34**, C9-285 (1973).
[20]J.-J. Rousseau, J.-Y. Gesland, M. Binois, and J. C. Fayet, C. R. Acad. Sci. Paris **279B**, 103 (1974).
[21]R. Yu. Abdulsabirov, L. D. Livanova, and V. G. Stepanov, Fiz. Tverd. Tela (Leningrad) **16**, 2135 (1974) [Sov. Phys.—Solid State **16**, 1395 (1975)].
[22]J. L. Patel, J. J. Davies, B. C. Cavenett, H. Takeuchi, and K. Horai, J. Phys. C **9**, 129 (1976).
[23]M. Arakawa and H. Ebisu, J. Phys. Soc. Jpn. **46**, 1571 (1979).
[24]H. Takeuchi and M. Arakawa, J. Phys. Soc. Jpn. **53**, 376 (1984).
[25]M. Arakawa, J. Phys. Soc. Jpn. **46**, 1245 (1979).
[26]P. Studzinski and J.-M. Spaeth, Phys. Status Solid B **136**, 735 (1986).
[27]J. J. Krebs and R. K. Jeck, Phys. Rev. B **5**, 3499 (1972).
[28]H. Murrieta S., F. J. Lopez, T. Rubio O., and G. Aguilar S., J. Phys. Soc. Jpn. **49**, 499 (1980).
[29]T. P. P. Hall, W. Hayes, R. W. H. Stevenson, and J. Wilkens, J. Chem. Phys. **38**, 1977 (1963).
[30]R. K. Jeck and J. J. Krebs, Phys. Rev. B **5**, 1677 (1972).
[31]J. J. Rousseau, M. Rousseau, and J. C. Fayet, Phys. Status Solidi **73**, 625 (1976).
[32]J. Rubio O., H. Murrieta S., and G. Aguilar S., J. Chem. Phys. **71**, 4112 (1979).
[33]R. C. DuVarney, J. R. Niklas, and J. M. Spaeth, Phys. Status Solid B **103**, 329 (1981).
[34]F. A. Modine, E. Sonder, W. P. Unruh, C. B. Finch, and R. D. Westbrook, Phys. Rev. B **10**, 1623 (1974).
[35]D. C. Stjern, R. C. DuVarney, and W. P. Unruh, Phys. Rev. B **10**, 1044 (1974).
[36]J. Y. Buzare and J. C. Fayet, Phys. Status Solid B **74**, 393 (1976).
[37]J. Y. Buzare and J. C. Fayet, Solid State Commun. **21**, 1097 (1977).
[38]H. Murrieta S., J. Rubio O., and G. Aguilar S., Phys. Rev. B **19**, 5516 (1979).
[39]M. Arakawa, J. Phys. Soc. Jpn. **47**, 523 (1979).
[40]J. Y. Buzare, J. C. Fayet, W. Berlinger, and K. A. Müller, Phys. Rev. Lett. **42**, 465 (1979).
[41]M. Fayet-Bonnel, J. Y. Buzare, and J. C. Fayet, Solid State Commun. **38**, 37 (1981).
[42]J. Y. Buzare, M. Fayet-Bonnel, and J. C. Fayet, J. Phys. C **14**, 67 (1981), and references therein.
[43]M. Arakawa and H. Ebisu, J. Phys. Soc. Jpn. **51**, 191 (1982).
[44]M. Arakawa, H. Aoki, H. Takeuchi, T. Yosida, and K. Horai, J. Phys. Soc. Jpn. **51**, 2459 (1982).

[45]M. Arakawa, H. Ebisu, and H. Takeuchi, J. Phys. Soc. Jpn. **54**, 3577 (1985).
[46]J. Y. Buzare, J. J. Rousseaum, and J. C. Fayet, J. Phys. (Paris) Lett. **38**, L445 (1977).
[47]J. Y. Buzare, J. C. Fayet, W. Berlinger, and K. A. Müller, Phys. Rev. Lett. **42**, 465 (1979).
[48]J. C. Fayet, Helv. Phys. Acta **58**, 76 (1985).
[49]M. Arakawa, H. Ebisu, T. Yosida, and K. Horai, J. Phys. Soc. Jpn. **46**, 1483 (1979).
[50]S. R. P. Smith and T. Cole, J. Chem. Phys. **52**, 1286 (1970).
[51]M. V. Vlasova, N. G. Kakazei, and L. A. Sorin, Kristallografiya **19**, 395 (1974) [Sov. Phys.—Crystallogr. **19**, 243 (1974)].
[52]E. J. Bijvank and H. W. den Hartog, Phys. Rev. B **12**, 4646 (1975).
[53]A. N. Lefferts, E. J. Bijvank, and H. W. den Hartog, Phys. Rev. B **17**, 4214 (1978).
[54]E. J. Bijvank, A. G. Zandbergen-Beishuizen, and H. W. den Hartog, Solid State Commun. **32**, 239 (1979).
[55]W. Low, Phys. Rev. **109**, 265 (1958).
[56]W. Low and R. S. Rubins, Phys. Lett. **1**, 316 (1962).
[57]A. Abragam and B. Bleaney, *Electron Paramagnetic Resonance of Transition Ions* (Oxford University Press, Oxford, 1970), p. 336.
[58]H. A. Buckmaster and Y. H. Shing, Phys. Status Solidi A **12**, 325 (1972).
[59]S. K. Misra and G. C. Upreti, J. Magn. Reson. Rev. **10**, 333 (1986).
[60]C. Rudowicz and R. Bramley, J. Chem. Phys. **83**, 5192 (1985).
[61]For a review, see N. Narayana, V. S. Sivasankar, and S. Radhakrishna, Phys. Status Solidi B **105**, 11 (1981).
[62]H. Murrieta S., G. Aquilar S., J. Rubio O., and E. Muñoz P., J. Chem. Phys. **61**, 2987 (1974).
[63]J. Rubio O. and W. K. Cory, J. Chem. Phys. **69**, 4792 (1978).
[64]U. Oseguera V., H. Murrietta S., C. Medrano P., J. Rubio O., and C. Ruiz-Mejia, J. Chem. Phys. **73**, 1132 (1980).
[65]A. Edgar and E. Siegel, J. Chem. Phys. **76**, 5657 (1982).
[66]M. Ikeya, Phys. Status Solidi B **111**, 525 (1982).
[67]M. T. Barriuso and M. Moreno, Phys. Rev. B **29**, 3623 (1984).
[68]G. D. Watkins, Phys. Rev. **113**, 79 (1959).
[69]V. M. Maevskii and E. N. Kalabukhova, Fiz. Tverd. Tela (Leningrad) **15**, 1622 (1973) [Sov. Phys.—Solid State **15**, 1090 (1973)].
[70]J. Rubio O., H. Murrieta S., E. Muñoz P., J. Boldú O., and G. Aquilar S., J. Chem. Phys. **63**, 4222 (1975).
[71]D. J. Newman, Aust. J. Phys. **29**, 263 (1976).
[72]J.-M. Moret and R. Lacroix, Helv. Phys. Acta **49**, 313 (1976).
[73]J. Boldú O., E. Muñoz P., W. K. Cory, and J. Rubio O., J. Chem. Phys. **67**, 2391 (1977).
[74]J. Rubio O., C. Rúiz-Mejia, U. Oseguera V., and H. Murrieta S., J. Chem. Phys. **73**, 53 (1980).
[75]K. Kawano, R. Nakata, and M. Sumita, Rep. Univ. Electro-Commun. **30**, 179 (1980).
[76]K. Kawano, R. Nakata, and M. Sumita, J. Phys. Soc. Jpn. **52**, 1402 (1983).
[77]R. Rohrig, Phys. Lett. **16**, 20 (1965).
[78]S. D. Pandey, J. Chem. Phys. **47**, 309 (1967).
[79]For a review, see B. Henderson and J. E. Wertz, Adv. Phys. **17**, 749 (1968).
[80]D. J. Newman and E. Siegel, J. Phys. C **9**, 4285 (1976).
[81]E. Siegel and K. A. Müller, Phys. Rev. B **19**, 109 (1979).
[82]K. A. Müller and W. Berlinger, J. Phys. C **16**, 6861 (1983).
[83]A. P. Pechenyi, M. D. Glinchuk, and V. N. Bliznyuk, Fiz. Tverd. Tela (Leningrad) **23**, 2121 (1981) [Sov. Phys.—Solid State **23**, 1237 (1981)].
[84]K. A. Müller, W. Berlinger, and J. Albers, Phys. Rev. B **32**, 5837 (1985).
[85]K. A. Müller and Th. von Waldkrich, in Local Properties at Phase Transitions, Proceedings of the International School of Physics "Enrico Fermi," Course LIX, Varenna, 1973, edited by K. A. Müller and A. Rigamonti (North-Holland, Amsterdam, 1976).